PHYSICAL REVIEW A VOLUME 8, NUMBER 6 DECEMBER 1973

# Multiple Inner-Shell Ionization of Aluminum by High-Velocity Medium-$Z$ Beams*

Forrest Hopkins,† D. O. Elliott, C. P. Bhalla,‡ and Patrick Richard
*Department of Physics, Kansas State University, Manhattan, Kansas 66506*
(Received 1 June 1973)

High-resolution studies of aluminum $K\alpha$ x rays produced by O, F, and Cl beams at beams energies $\gtrsim 1$ MeV/amu have been performed with a crystal spectrometer. Fluorescence yields are calculated for the various single $K$-shell, multiple $L$-shell vacancy configurations. A simple model of the ionization process has been assumed that allows determination of average $2s$ and $2p$ ionization probabilities from the experimental x-ray yields using the calculated fluorescence yields.

## I. INTRODUCTION

The $K\alpha$ x-ray satellite structure for aluminum arising from bombardment by high-velocity beams has been studied recently. X-ray intensities from the Al single $K$-shell, multiple $L$-shell vacancies produced by 0.4–10.0-MeV helium ions have been measured.[1,2] The satellite structure for 5.0-MeV nitrogen incident on aluminum has been reported.[3] Knudson, Nagel, and Burkhalter[4] have studied the same set of x rays as produced by neon beams between 1.5 and 15.0 MeV in energy. The relative intensities at several energies were recorded for the various satellite groups. Measurements have also been made for oxygen incident on aluminum over a wide range of bombarding energies.[5] The purpose of the present work is to extend the $Z$ values of the bombarding projectiles and to determine the relative x-ray production ratios for the Al defect configurations. Ionization probabilities are extracted from these ratios and compared to predictions of the binary-encounter theory[6] assuming uncorrelated electrons.

Section II contains the experimental procedure, followed by a discussion of the observed x-ray yields in Sec. III. A brief description of the procedure used in obtaining ionization probabilities is given in Sec. IV. The theoretical fluorescence yields, calculated with the Hartree-Fock-Slater model are presented in Sec. V. Combining the experimental and theoretical results of Secs. III–V the experimental ionization probabilities are deduced from the data in Sec. VI. Section VII contains calculations using particular values of the extracted probabilities and a concluding discussion constitutes Sec. VIII.

## II. EXPERIMENTAL PROCEDURE

The beams used in this experiment were produced by the Kansas State University tandem Van de Graaff. A 30-MeV $O^{(5+)}$ beam was focused onto quartz with no collimation. The target was a thick aluminum foil placed at 45° with respect to the beam. Beam integration on the target determined the period of accumulation of counts at each spectrometer setting. A 4-in. curved crystal vacuum spectrometer equipped with an ammonium dihydrogen phosphate (ADP) crystal was used to analyze the x rays. The crystal was stepped 0.059 mÅ per accumulation period under computer control. The efficiency of the spectrometer was assumed constant over the small range of wavelengths studied. A horizontal entrance slit 0.01 in. in width and 0.5 in. in length collimated the x rays as did an 0.02-in.-wide slit just before a proportional counter. A 2 $\mu$ (Markrofol) foil was used as the window of the proportional counter, which was operated with a 10% methane-90% argon gas mixture at one atmosphere of pressure. A bias of 2000 V was applied to the counter. A single-channel analyzer window was set on the counter output and the resulting logic signal fed to the computer. The position of the beamspot was checked before and after the run by replacing the target with the quartz.

Similar scans were made with a fluorine ($F^{5+}$) beam of 30 MeV incident on the thick aluminum target and with chlorine beams of energies 29.12 MeV ($Cl^{5+}$), 35.00 MeV ($Cl^{6+}$), and 40 MeV ($Cl^{7+}$). In addition, a thin target measurement using the 29.12-MeV Cl beam was performed with a thin aluminum film on a thick copper foil. The thickness of the aluminum was estimated by means of an interferometer to be at most 200 Å or about 5 $\mu g/cm^2$. The energy loss of a 29-MeV Cl beam over such a thickness is expected to be less than 0.1 MeV. The intent of this measurement was to observe the possible effects of the thick target on the spectra due to energy degradation of the beam and self-absorption of $K\alpha$ x rays in the target for the chlorine case.

## III. EXPERIMENTAL X-RAY YIELDS

The Al $K\alpha$ x-ray spectrum for chlorine ions incident on the thin aluminum target is shown in Fig. 1. Scans above and below the energy region of the satellite peaks gave an indication of background. The energies for the $K\alpha$ satellite groups are compared to previous experimental and theoretical values in Table I. The thick target spectra presented in Fig. 2 reveal little difference qualitatively from the thin target spectrum. The ratios of the intensities in the thick and thin target cases are essentially the same, as can be seen in Table II, implying negligible corrections in the intensity ratios for the three Cl spectra taken with thick targets.

The only noticeable difference in the thin target spectrum is the indication of a seventh peak at 1562 eV, approximately the energy expected for either a $K\alpha$ x ray arising from an initial configuration with only two $L$-shell electrons in addition to a single $K$-shell electron or a $K\beta$ x ray arising from an initial configuration with a single $K$-shell vacancy. The intensity of this peak relative to the $K\alpha$ lines suggests the former origin to be the correct one. The thick target spectra fail to show such a peak due to the fact that the $K$ absorption edge for Al lies at 1559 eV and x rays of the energy of the seventh group produced at any depth in the target are greatly attenuated. In a thick target spectrum, this effect would greatly lessen the intensity of the peak relative to the lower energy peaks as a substantial amount of the ionization presumably occurs at depths greater than 200 Å.

The ratio of the x-ray yields, $\sigma^X_{1K,nL}$, to the total x-ray yield, $\sigma^X_K$, for the six prominent satellite peaks are listed in Table II. No thick target corrections were applied to the ratios.

TABLE I. Energies of Al $K\alpha$ satellite x-rays compared to calculations for the electronic configurations: $(1s)^1(2s)^2(2p)^q(3s)^2(3p)^1$.

| $q$ | $E_{meas}$ (eV) | $E_{meas}$ [a] (eV) | $E_{theor}$ [b] (eV) |
|---|---|---|---|
| 6 | 1486±1 | 1486 | 1485 |
| 5 | 1496±1 | 1496 | 1494 |
| 4 | 1507±1 | 1507 | 1505 |
| 3 | 1519±1 | 1521 | 1517 |
| 2 | 1532±1 | 1534 | 1531 |
| 1 | 1545±1 | 1548 | 1547 |

[a] Previous experimental results from Ref. 3.

[b] Calculated by the authors using the Hartree-Fock-Slater model with HOVD exchange approximation.

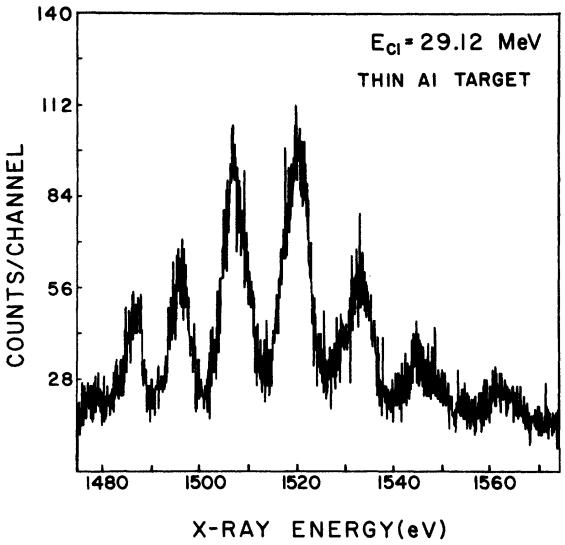


FIG. 1. Al $K\alpha$ satellite x-ray spectrum produced by a 29.12-MeV Cl beam incident on a thin Al target.

## IV. EMPIRICAL DETERMINATION OF IONIZATION PROBABILITIES

The ionization cross section $\sigma_j$ can be expressed as the integral of the probability, $P_j(b)$, for single ionization for a shell with $N_j$ electrons, over the impact parameter $b$,[7]

$$\sigma_j = N_j \int_0^\infty 2\pi b P_j(b)\, db\,. \tag{1}$$

Assuming independent events, the cross section for the simultaneous production of one $K$-shell and $n$ $L$-shell vacancies, $\sigma^I_{1K,nL}$, may be expressed as[1,8]

$$\sigma^I_{1K,nL} = N_K \int_0^\infty 2\pi b P_K(b) P_{nL}(b)\, db\,, \tag{2}$$

where $P_K(b)$ and $P_{nL}(b)$ are the probabilities for single $K$-shell ionization and multiple $L$-shell ionization, respectively.

TABLE II. Ratio, $\sigma^X_{K,nL}/\sigma^X_K$, of yields [a] for Al $K\alpha$ satellites with $n$ $L$-shell electron vacancies.

| Beam | Energy (MeV) | $n=0$ | $n=1$ | $n=2$ | $n=3$ | $n=4$ | $n=5$ |
|---|---|---|---|---|---|---|---|
| $^{16}$O | 30.0 | 0.087 | 0.181 | 0.262 | 0.308 | 0.106 | 0.063 |
| $^{19}$F | 30.0 | 0.068 | 0.141 | 0.320 | 0.310 | 0.111 | 0.050 |
| $^{35}$Cl (thick) | 29.12 | 0.086 | 0.130 | 0.208 | 0.246 | 0.206 | 0.124 |
| $^{35}$Cl (thin) | 29.12 | 0.080 | 0.121 | 0.256 | 0.294 | 0.167 | 0.083 |
| $^{35}$Cl | 35.0 | 0.094 | 0.135 | 0.222 | 0.249 | 0.184 | 0.116 |
| $^{35}$Cl | 40.0 | 0.076 | 0.107 | 0.206 | 0.257 | 0.209 | 0.145 |

[a] Statistical errors for the intensities were at most 10% and typically much smaller.

In Eq. 2 no distinction is made between $L$-shell vacancies in the $2s$ and $2p$ subshells. Since the ionization probabilities for the subshells are different and the fluorescence yields for configurations in the $L$ shell depend on the relative population of $2s$ and $2p$ electrons, the ionization cross section must include the specific configurations. Consequently, the cross section, $\sigma^I_{Kij}$, for the production of a particular configuration with one $K$-shell vacancy, $i$ vacancies in the $2s$ subshell, and $j$ vacancies in the $2p$ subshell, can be expressed as[9]

$$\sigma^I_{Kij} = N_K \int_0^\infty 2\pi b P_K(b) P_{ij}(b)\, db\,, \tag{3}$$

where $i+j=n$, the total number of the $L$-shell vacancies. The quantity $P_{ij}$ can be represented by

$$P_{ij}(b) = C\binom{2}{i}[P_{2s}(b)]^i[1-P_{2s}(b)]^{2-i} \times C\binom{6}{j}[P_{2p}(b)]^j[1-P_{2p}(b)]^{6-j}\,, \tag{4}$$

where $P_{2s}(b)$ and $P_{2p}(b)$ are the probabilities of ejecting one electron from the $2s$ and $2p$ subshells, respectively, for an impact parameter $b$.

The quantities $C\binom{n}{n}$ are the binomial coefficients. The assumption of independent events for the $2s$ and $2p$ electrons is made here.

The $K\alpha$ transition for different configurations with $n$ $L$-shell vacancies but different populations in the $2s$ and $2p$ subshells cannot be resolved in the present experiment. Therefore an Al satellite peak in our spectrum will consist of all configurations with the same number of $L$-shell vacancies. The total x-ray production cross section for a particular $K\alpha$ satellite peak will then be given by

$$\sigma^X_{K,nL} = \sum_{ij} \sigma^I_{Kij}\,\omega_{ij}\,, \quad \text{with } i+j=n\,, \tag{5}$$

where $\omega_{ij}$ is the fluorescence yield for the configuration with one $K$-shell vacancy, $i$ $2s$ vacancies, and $j$ $2p$ vacancies. Equation (5) has one term for $n=0$ and 7; two terms for $n=1$ and 6; and three terms for $n=2$, 3, 4, and 5. A restriction is made here that no $L_1L_{23}M$ Coster-Kronig transition can occur for these configurations, as will be discussed in Sec. V. The ratio of $\sigma^X_{1K,nL}$ to the total $K\alpha$ x-ray production cross section $\sigma^X_K$ can be expressed in terms of probabilities by

$$\frac{\sigma^X_{K,nL}}{\sigma^X_K} = \sum_{ij}\left[\int_0^\infty 2\pi b P_K(b) P_{ij}(b)\, db\right]\omega_{ij} \Big/ \sum_{n=0}^{7}\sum_{ij}\left[\int_0^\infty 2\pi b P_K(b) P_{ij}(b)\, db\right]\omega_{ij}\,. \tag{6}$$

In this experiment the parent $K\alpha$ peak plus five $K\alpha$ satellite peaks, $n=1,\ldots,5$, constitute essentially all of the observed $K\alpha$ x rays.

The dominant contribution of single $K$-shell, multiple $L$-shell ionization is from impact parameters small compared to the $L$-shell radii.[9] This is due to the fact that $P_K$ is essentially zero for $b$ greater than the $K$-shell radius. This has recently been experimentally verified for high-energy heavy ion collisions.[10] Calculations[8,9] demonstrate that $P_{2s}(b)$ and $P_{2p}(b)$ are approximately constant, over the range of $b$ for which $P_K(b) \neq 0$. The quantities $P_{2s}$ and $P_{2p}$ and thus $P_{ij}$ are defined as the average ionization probabilities for small impact parameters. With these considerations Eq. 6 becomes

$$\frac{\sigma^X_{K,nL}}{\sigma^X_K} = \sum_{ij} P_{ij}\,\omega_{ij} \Big/ \sum_{n=0}^{7}\sum_{ij} P_{ij}\,\omega_{ij}\,. \tag{7}$$

This equation is used to determine the average ionization probabilities $P_{2s}$ and $P_{2p}$ which fit the data. The left-hand side of Eq. 7 is given by the six experimental ratios for $n=0$, 1, 2, 3, 4, and 5 as given in Table II. The right-hand side of the equation contains two quantities $P_{2s}$ and $P_{2p}$ and the fluorescence yields. Theoretical fluorescence yields as described in Sec. V are used in the equation. For fixed values of the ratio $P_{2s}/P_{2p}$ between 0.2 and 5.0, a least-squares fit to the experimental ratios is made by varying the single parameter $P_{2p}$.

## V. CALCULATIONS OF FLUORESCENCE YIELDS

The $K\alpha$ fluorescence yield for a vacancy in the $K$ shell is defined as

$$\omega_{K\alpha} = \frac{T_X(2p-1s)}{\Gamma_X+\Gamma_A}\,,$$

where $T_X(2p-1s)$ is the $K\alpha$ x-ray rate and $\Gamma_X$ and $\Gamma_A$ are the total x-ray and total Auger transition rates. The standard theoretical values[11] of $\omega_K$ correspond to fluorescence yields in an atom with a single vacancy in the $K$ shell.[12] Specific fluorescence yields appropriate to multiple vacancy configurations have been reported for two cases.[13,14] In addition, the scaling procedure by Larkins[15] provides for the approximation of the fluorescence yields for multiply ionized states.

The Auger group rate for the transition involving two electrons, which are initially described by

$n_1l_1$ and $n_2l_2$ quantum numbers, filling a vacancy $(n_3l_3)$ and resulting in one electron in the continuum, $El_4$, is given in atomic units ($\hbar = m = e = 1$) by

$$T_A(n_3l_3 \rightarrow n_1l_1n_2l_2) = 2\pi N_{12} \sum_{L,S} \frac{(2S+1)(2L+1)}{2(2l_3+1)} \sum_{l_4} |M|^2, \quad (8)$$

where the quantum numbers $L, S, J$ refer to the final state. The weighting factor $N_{12}$ is given in terms of the occupation numbers $N_1$ and $N_2$, respectively, for the $n_1l_1$ and the $n_2l_2$ orbitals.

$$N_{12} = \begin{cases} \dfrac{N_1N_2}{(4l_1+2)(4l_2+2)} & \text{for inequivalent electrons} \\ \dfrac{N_1(N_1-1)}{(4l_1+2)(4l_1+2-1)} & \text{for equivalent electrons } (n_1=n_2, l_1=l_2). \end{cases}$$

The matrix element $M$ in Eq. (8) is defined as

$$M \equiv \langle \phi(n_3l_3, El_4L'S'J'M') | 1/r_{12} | \phi(n_1l_1, n_2l_2LSJM) \rangle, \quad (9)$$

where $\phi$ represents the antisymmetrized wave function. The explicit reduction of $M$ is given elsewhere.[11]

The x-ray transition rate, in the electric dipole approximation, is given (in atomic units) by

$$T_x = \tfrac{4}{3} k^3 [l_> /(2l_i+1)] |\langle n_f l_f | r | n_i l_i \rangle|^2. \quad (10)$$

The value of $k$ in our units is equal to the x-ray transition energy divided by $c$. The above rate is reduced by the ratio of the number of electrons in the $n_f l_f$ orbital to the maximum possible number of electrons in this orbital $[=2(2l_f+1)]$.

The present calculations of the Auger group rates and the x-ray rates were performed with the Hartree-Fock-Slater model, with the exchange approximation[16] of Herman, Ortenburger, and Van Dyke (HOVD). The calculated rates, $K$-$LL$, $K$-$LM$, and $K$-$MM$ and the total Auger rate of Al, are given in Table III for electronic configurations $(1s)(2s)^{2-i}(2p)^{6-j}(3s)^2(3p)$ for $i = 0, 1, 2$, and $j = 0, 1, 2, 3, 4, 5$. For the same configurations, the $K\alpha$ and total $K$ x-ray rates and the resulting values $\omega_{K\alpha}$ and $\omega_K$ are also listed in Table III. The total $K$ x-ray rate is simply the sum of the $K\alpha$ and $K\beta$ rates with the assumption of three electrons in the $M$ shell. Of course many defect configurations will in fact include fewer than three such electrons, but the $K\beta$ rates as calculated are already small compared to the corresponding $K\alpha$ rates. We note that the $K$-$MM$ Auger rate is at most 1.9% of the total Auger rate for the defect configuration $[1s^1, 2p^5]$ and its contribution decreases for less-highly-stripped cases ($\approx 0.1\%$ for $[1s^1, 2p^1]$).

In this paper it is assumed that a vacancy in the $2s$ subshell is not filled by an $L_1L_{23}M$ Coster-Kronig transition. Calculations show that this transition is energetically allowed only for the four electronic defect configurations $[2s]$, $[2s, 2p]$, $[2s, 2p^2]$, and $[1s, 2s]$. Only the last defect configuration involves a $K$-shell vacancy, which is required for obtaining a $K\alpha$ transition as observed in the present experiment. We have neglected this one case in the analysis since the fluorescence yield for the two defect configurations $[1s, 2s]$ and $[1s, 2p, 3p]$ differ by only about 12%.

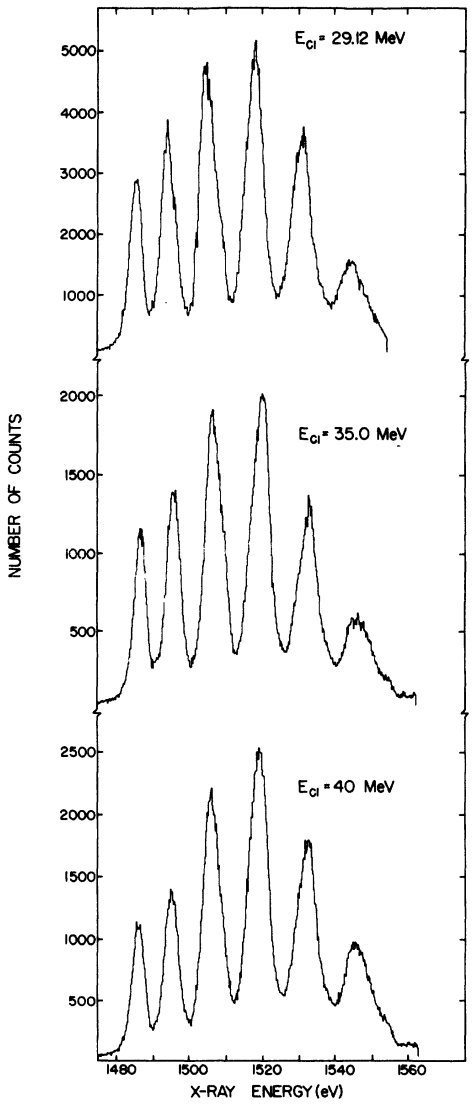


FIG. 2. Al $K\alpha$ satellite x-ray spectra produced by Cl beams incident on thick Al targets at bombarding energies of 29.12, 35.0, and 40.0 MeV.

TABLE III. Calculated transition rates and fluorescence yields for Al.

| Electronic configuration | Rates ($10^3$/a.u.) K-LL | K-LM | K-MM | Total Auger | Kα x ray | Total x ray | $\omega_{K\alpha}$ | $\omega_K$ |
|---|---|---|---|---|---|---|---|---|
| $(1s)^1(2s)^2(2p)^6(3s)^2(3p)^1$ | 12.693 | 0.523 | 0.007 | 13.222 | 0.560 | 0.565 | 0.041 | 0.041 |
| $(1s)^1(2s)^2(2p)^5(3s)^2(3p)^1$ | 10.696 | 0.731 | 0.015 | 11.441 | 0.505 | 0.513 | 0.042 | 0.043 |
| $(1s)^1(2s)^2(2p)^4(3s)^2(3p)^1$ | 8.537 | 0.901 | 0.025 | 9.462 | 0.437 | 0.447 | 0.044 | 0.045 |
| $(1s)^1(2s)^2(2p)^3(3s)^2(3p)^1$ | 6.360 | 1.024 | 0.039 | 7.742 | 0.353 | 0.368 | 0.044 | 0.047 |
| $(1s)^1(2s)^2(2p)^2(3s)^2(3p)^1$ | 4.368 | 1.079 | 0.056 | 5.503 | 0.254 | 0.272 | 0.044 | 0.047 |
| $(1s)^1(2s)^2(2p)^1(3s)^2(3p)^1$ | 2.804 | 1.053 | 0.075 | 3.932 | 0.136 | 0.159 | 0.033 | 0.039 |
| $(1s)^1(2s)^1(2p)^6(3s)^2(3p)^1$ | 11.108 | 0.676 | 0.004 | 11.787 | 0.599 | 0.608 | 0.048 | 0.049 |
| $(1s)^1(2s)^1(2p)^5(3s)^2(3p)^1$ | 8.797 | 0.832 | 0.008 | 9.638 | 0.539 | 0.551 | 0.053 | 0.054 |
| $(1s)^1(2s)^1(2p)^4(3s)^2(3p)^1$ | 6.381 | 0.938 | 0.012 | 7.333 | 0.477 | 0.494 | 0.061 | 0.063 |
| $(1s)^1(2s)^1(2p)^3(3s)^2(3p)^1$ | 4.039 | 0.976 | 0.018 | 5.032 | 0.375 | 0.396 | 0.069 | 0.073 |
| $(1s)^1(2s)^1(2p)^2(3s)^2(3p)^1$ | 2.001 | 0.932 | 0.025 | 2.957 | 0.269 | 0.294 | 0.083 | 0.091 |
| $(1s)^1(2s)^1(2p)^1(3s)^2(3p)^1$ | 0.546 | 0.792 | 0.098 | 1.436 | 0.144 | 0.174 | 0.089 | 0.108 |
| $(1s)^1(2s)^0(2p)^6(3s)^2(3p)^1$ | 10.310 | 0.764 | 0.025 | 11.100 | 0.641 | 0.654 | 0.055 | 0.056 |
| $(1s)^1(2s)^0(2p)^5(3s)^2(3p)^1$ | 7.821 | 0.852 | 0.039 | 8.712 | 0.576 | 0.593 | 0.062 | 0.064 |
| $(1s)^1(2s)^0(2p)^4(3s)^2(3p)^1$ | 5.313 | 0.872 | 0.056 | 6.240 | 0.497 | 0.518 | 0.074 | 0.077 |
| $(1s)^1(2s)^0(2p)^3(3s)^2(3p)^1$ | 2.995 | 0.809 | 0.064 | 3.868 | 0.401 | 0.426 | 0.093 | 0.099 |
| $(1s)^1(2s)^0(2p)^2(3s)^2(3p)^1$ | 1.123 | 0.652 | 0.099 | 1.874 | 0.287 | 0.317 | 0.131 | 0.145 |
| $(1s)^1(2s)^0(2p)^1(3s)^2(3p)^1$ | ··· | 0.389 | 0.127 | 0.516 | 0.154 | 0.189 | 0.218 | 0.268 |

## VI. EXPERIMENTAL IONIZATION PROBABILITIES

Using Eq. (7), the experimental ratios from Table II, the calculated $K\alpha$ fluorescence yields in Table III, and fixed values of the ratio $R$ of $P_{2s}$ to $P_{2p}$, the best least-squares fit to $P_{2p}$ have been obtained. In Table IV the best fit values of $P_{2p}$ are given for various values of the ratio $R$. For $R$ less than 0.3 or greater than 2.0, the fits were poor. The striking feature of the results in each case is the lack of variation of the probability $P_{2p}$ over a wide range of values for $R$, that is, widely differing values for $P_{2s}$. Total changes in $P_{2p}$ are about 20% from $R=0.3$ to $R=1.0$. The fits presented are all of comparable quality and so provide no basis for selection of one average set of probabilities, $P_{2s}$ and $P_{2p}$, for the set of yields in every case. However, in spite of the large uncertainty in $P_{2s}$, the quantity $P_{2p}$ is fairly well determined in each case. The 29-MeV Cl data on the thin Al target are not given in the table. A best least-squares-fit value of 0.367 is obtained for $P_{2p}$ with $R=0.5$. The thin target value of $P_{2p}$ is thus 7.5% smaller than the thick target value.

A prediction of the binary encounter theory for single ionization in Al is that the probability $P_{2s}$ is approximately one-half of $P_{2p}$. This corresponds to a value of $R=0.5$ in Table IV, for which $P_{2p}$ is 0.33 and 0.40 for the oxygen and chlorine

TABLE IV. Best-fit [a] values of $P_{2p}$ for various values of $R(=P_{2s}/P_{2p})$.

| $R=\frac{P_{2s}}{P_{2p}}$ | O | $X^2$ | F | $X^2$ | Cl (29 MeV) | $X^2$ | Cl (35 MeV) | $X^2$ | Cl (40 MeV) | $X^2$ |
|---|---|---|---|---|---|---|---|---|---|---|
| 0.3 | 0.354 | 1.28 | 0.360 | 1.20 | 0.428 | 1.79 | 0.409 | 1.79 | 0.447 | 1.46 |
| 0.4 | 0.341 | 1.26 | 0.346 | 1.31 | 0.412 | 1.58 | 0.393 | 1.58 | 0.430 | 1.25 |
| 0.5 | 0.328 | 1.25 | 0.334 | 1.40 | 0.397 | 1.44 | 0.379 | 1.45 | 0.414 | 1.13 |
| 0.6 | 0.317 | 1.24 | 0.322 | 1.47 | 0.383 | 1.34 | 0.366 | 1.36 | 0.400 | 1.04 |
| 0.7 | 0.307 | 1.23 | 0.312 | 1.52 | 0.370 | 1.28 | 0.354 | 1.30 | 0.387 | 0.99 |
| 0.8 | 0.297 | 1.22 | 0.302 | 1.55 | 0.359 | 1.25 | 0.343 | 1.26 | 0.375 | 0.96 |
| 0.9 | 0.289 | 1.21 | 0.293 | 1.55 | 0.348 | 1.23 | 0.333 | 1.25 | 0.364 | 0.95 |
| 1.0 | 0.280 | 1.21 | 0.285 | 1.55 | 0.339 | 1.22 | 0.324 | 1.24 | 0.354 | 0.94 |
| 2.0 | 0.222 | 1.19 | 0.226 | 1.27 | 0.269 | 1.66 | 0.257 | 1.65 | 0.281 | 1.31 |

[a] The quantity $X^2$ is a sum of the differences between the six measured and calculated ratios divided by the weighting factor 0.005.

TABLE V. Calculations with $P_{2p}$ ($R=0.5$) for electronic configurations $(1s)(2s)^{2-i}(2p)^{6-j}-(3s)^2(3p)$.

| | Vacancies | | Oxygen | | | | Chlorine (29 MeV) | | | |
|---|---|---|---|---|---|---|---|---|---|---|
| $n$ | $i$ | $j$ | $\sigma^I_{Kij}/\sigma^I_{K00}$ | $Y_{ij}$ | $Y_n$ | $Y_{\text{expt}}$ | $\sigma^I_{Kij}/\sigma^I_{K00}$ | $Y_{ij}$ | $Y_n$ | $Y_{\text{expt}}$ |
| 0 | 0 | 0 | 1.00 | 0.054 | 0.054 | 0.087 | 1.00 | 0.025 | 0.025 | 0.086 |
| 1 | 1 | 0 | 0.40 | 0.025 | 0.187 | 0.181 | 0.50 | 0.014 | 0.115 | 0.130 |
| | 0 | 1 | 2.95 | 0.162 | | | 4.00 | 0.101 | | |
| | 2 | 0 | 0.03 | 0.003 | | | 0.07 | 0.002 | | |
| 2 | 1 | 1 | 0.75 | 0.081 | 0.293 | 0.262 | 2.00 | 0.064 | 0.242 | 0.208 |
| | 0 | 2 | 3.65 | 0.209 | | | 6.63 | 0.176 | | |
| | 2 | 1 | 0.11 | 0.011 | | | 0.23 | 0.011 | | |
| 3 | 1 | 2 | 1.43 | 0.114 | 0.253 | 0.307 | 3.33 | 0.122 | 0.289 | 0.246 |
| | 0 | 3 | 2.38 | 0.128 | | | 5.90 | 0.156 | | |
| | 2 | 2 | 0.14 | 0.014 | | | 0.40 | 0.019 | | |
| 4 | 1 | 3 | 0.95 | 0.084 | 0.149 | 0.106 | 2.97 | 0.122 | 0.219 | 0.206 |
| | 0 | 4 | 0.89 | 0.051 | | | 2.97 | 0.078 | | |
| | 2 | 3 | 0.10 | 0.012 | | | 0.37 | 0.022 | | |
| 5 | 1 | 4 | 0.35 | 0.038 | 0.057 | 0.063 | 1.47 | 0.074 | 0.112 | 0.124 |
| | 0 | 5 | 0.17 | 0.007 | | | 0.80 | 0.016 | | |

(29 MeV) data, respectively. Using these values of $P_{2p}$ and $P_{2s}$, three quantities of interest can be calculated. The first are the ratios of the individual ionization cross sections, $\sigma^I_{Kij}$, to the cross section for a single $K$-shell ionization only, $\sigma^I_{K00}$:

$$\frac{\sigma^I_{Kij}}{\sigma^I_{K00}}=\frac{P_{ij}}{P_{00}}. \tag{11}$$

The second set of calculations are for the ratio of x-ray yields resulting from each configuration, denoted

$$Y_{Kij}=P_{ij}\omega_{ij}\Big/\sum_{n=0}\sum_{ij}P_{ij}\omega_{ij}\ .$$

The third quantity $Y_n$ is the sum of the contributions for particular satellite groups [$Y_n=\sum_{ij}Y_{Kij}$; see Eq. (7)]. These three quantities along with the data $Y_{\text{expt}}$ are presented in Table V.

The agreement between the ratio of yields $Y_n$ and $Y_{\text{expt}}$ is good, except for the parent $K\alpha$ line. The accuracy of the fits presented is typical for other values of $R$ and also for the sets of data for F, Cl (35 MeV), and Cl (40 MeV). The interesting feature of the relative ionization cross sections $\sigma^I_{Kij}/\sigma^I_{K00}$ is that as the total number, $n$, of $L$-shell electrons stripped is increased, the ionization cross section for the configuration with one $2s$ vacancy surpasses that for the configuration with no $2s$ vacancies (for the same value of $n$). Only for $n=5$ do the configurations with two $2s$ vacancies become comparable to those for no $2s$ vacancies. The x-ray yield for two ($2s$) vacancies is actually greater than that for no ($2s$) vacancies for $n=5$ due to the differences in fluorescence yield.

The purpose of the information in Table V is to demonstrate the relative contributions to the ionization and x-ray production processes for a reasonable set of values for $P_{2s}$ and $P_{2p}$. It must be stressed that the data itself provide no basis for the selection of a unique set.

TABLE VI. Comparison of theoretical and experimentally obtained values for $P_{2p}$.

| Projectile | O | F | Cl(29 MeV) | Cl(35 MeV) | Cl(40 MeV) |
|---|---|---|---|---|---|
| BEA | 1.125 | 1.708 | 10.487 | 9.070 | 8.474 |
| Expt | 0.328 | 0.334 | 0.397 | 0.379 | 0.414 |

## VII. COMPARISON WITH THEORY OF IONIZATION

In Sec. VI we have obtained the quantities $P_{2s}$ and $P_{2p}$ from the experimental data and the model of independent probabilities for multiple ionization. In this model $P_{2s}$ and $P_{2p}$ represent the average ionization probabilities for the $2s$ and $2p$ subshells, respectively, at small values of $b$ where $P_K(b)\neq 0$. In this section the calculation of $P_{2p}$ based on the binary encounter model[6] is presented and compared to experiment.

The $2p$ subshell ionization cross section in the binary encounter model is given by[8,17]

$$\sigma_{2p}=\frac{N_{2p}Z_1^2\sigma_0}{U_{2p}^2}G\left(\frac{V_{\text{inc}}}{V_{\text{orb}}}\right), \tag{12}$$

where $Z_1$ is the atomic number of the projectile, $N_{2p}$ is the number of electrons in the $2p$ shell, $U_{2p}$ is the $2p$-shell electron binding energy, $\sigma_0=6.56\times10^{-14}$ cm$^2$ eV$^2$, $V_{\text{inc}}$ is the projectile velocity, and $V_{\text{orb}}$ is the velocity of the electron. The

values for $G(V_{inc}/V_{orb})$, which depend solely on the ratio of velocities, are taken from Ref. 8. The probability for single ionization at zero impact parameter of a given shell can be represented as[8,17]

$$P_{2p}(0)=\frac{\sigma_{2p}/N_{2p}}{2\pi\langle r_{2p}^2\rangle}, \tag{13}$$

where $\langle r_{2p}^2\rangle$ is the rms radius of the $L$ shell. Combining Eqs. (12) and (13), the values of $P_{2p}(0)$ can be calculated for any target-projectile combination and incident ion energy. In particular they have been calculated for the five cases listed in Table VI, and compared to the fits for $R=0.5$, the value for the ratio predicted by the theory. In the calculation, $\langle r_{2p}^2\rangle$ is calculated with the Hartree-Fock-Slater model, the normal $2p$-shell binding energy is used for $U_{2p}$, and the bare nuclear charge of the projectile is used for $Z_1$ in each case.

The procedure used above to compare experimental data and theory has been successful in cases where light projectiles were used, specifically protons and $\alpha$ particles incident on various targets.[2,18] It is apparent, however, that fundamental difficulties arise with higher $Z$ projectiles as is evident from Table VI. The BEA theory does predict quite well total $L$-shell cross sections for protons bombarding heavy targets.[19,20] The assumptions made in relating the average $L$-shell ionization probability to the theoretical probability at zero impact parameter, i.e., Eq. (13), may oversimplify the picture for a projectile with high $Z$ value. In particular, an integration of Eq. (2) using explicit functions of $b$ for $P_k$ and $P_{nL}$ would result in a more exact quantity for comparison.

In addition, the parameters $U_{2p}, \langle r_{2p}^2\rangle, Z_1$, and $V_{orb}$ are not uniquely defined in an ion-atom collision, especially for near zero impact parameters. Since $U_{2p}$ is so small, the large value of $Z_1$ may cause $U_{2p}$ to increase substantially, which leads to a decreased value of $P_{2p}(0)$. An increased binding effect due to a combined target and projectile nuclear charge has been suggested by Basbas *et al.*[21] for projectile velocities much lower than orbital electron velocities. For large $Z_1$ this effect may be important even for projectile velocities comparable to the orbital electron velocities. The resolution of questions of this type are necessary before the explanation of the discrepancies in Table VI can reasonably be attempted.

## VIII. DISCUSSION AND CONCLUSIONS

High-resolution Al $K\alpha$ x-ray spectra produced by oxygen, fluorine, and chlorine beams are presented and the experimental ratios $\sigma^X_{1K,nL}/\sigma^X_K$ determined. Using the assumption of independent ionization probabilities, the experimental data were used to obtain average $2s$ shell and $2p$ shell probabilities per electron near zero impact parameter for Al. The fluorescence yields needed in this analysis were calculated for the defect configurations of Al.

The results of this work can be compared with previous data. Values for average $L$-shell probabilities have been determined previously for He + Al[2] and O + Al[5], both at an MeV/amu bombarding energy, using Eq. (2) and a method otherwise similar to the one presented in this paper. The probability $P_{nL}$ in this approach is given by

$$P_{nL}=C\binom{8}{n}P_L^n(1-P_L)^{8-n}.$$

Although no distinction was made in those analyses between $2s$ shell and $2p$ shell ionization, a comparison is still informative. The average $P_{2p}$ values obtained here for $R=1$ ($P_{2s}=P_{2p}$) might be expected to be close to the total average $L$-shell values $P_L$. The $P_L$ for He + Al[2] was approximately 0.08 and that for O + Al[5] was about 0.38. The present chlorine data for 35-MeV bombarding energy and $R=1.0$. resulted in a $P_{2p}$ value of 0.324. Since these three cases were all for bombarding energies of 1 MeV/amu, it is apparent that the amount of multiple $L$-shell ionization increases dramatically in going from projectile $Z=2$ to $Z=8$ and then levels off somewhat from $Z=8$ to $Z=17$.

It is also possible to compare the two methods of analysis for the case of O + Al at ~2 MeV/amu. From Ref. 5 a value of $P_L=0.32$ was obtained assuming Coster-Kronig transitions transfer $2s$ holes to the $2p$ shell. With $R=1$, the present analysis yields $P_{2p}=0.28$ compared to a value of 0.328 for $R=0.5$.

## ACKNOWLEDGMENTS

The help of Keith Jamison and Cliff Woods in taking and analyzing the data is gratefully acknowledged.

---

*Work supported in part by the U.S. Atomic Energy Commission.

†Present address: Physics Department, SUNY, Stony Brook, L.I., New York.

‡Work supported in part by the U.S. Army Research Office, Durham, N. Carolina.

[1] A. R. Knudson, P. G. Berkhalter, and D. J. Nagel, U.S. Atomic Energy Commission Report CONF-720404,

1973 (unpublished).
[2]Patrick Richard, R. L. Kauffman, J. H. McGuire, C. Fred Moore, and David Olsen, Phys. Rev. A 8, 1369 (1973).
[3]A. R. Knudson, D. J. Nagel, P. G. Berkhalter, and K. L. Dunning, Phys. Rev. Lett. 26, 1149 (1971).
[4]A. R. Knudson, D. J. Nagel, and P. G. Berkhalter, Phys. Lett. A42, 69 (1972).
[5]David K. Olsen, C. Fred Moore, and R. L. Kauffman, Phys. Lett. A44, 109 (1973).
[6]J. D. Garcia, Phys. Rev. A 1, 280 (1970); Phys. Rev. A 4, 955 (1971).
[7]J. Bang and J. M. Hansteen, K. Dan. Vidensk. Selsk. Mat.-Fys. Medd. 31, No. 13 (1959).
[8]James H. McGuire and Patrick Richard, Bull. Am. Phys. Soc. 18, 662 (1973); Phys. Rev. A 8, 1374 (1973).
[9]J. M. Hansteen and O. P. Mosebekk, Phys. Rev. Lett. 29, 1361 (1972).
[10]C. L. Cocke and R. Randall, Phys. Rev. Lett. 30, 1016 (1973).
[11]D. L. Walters and C. P. Bhalla, Phys. Rev. A 3, 1919 (1971); Atomic Data 3, 301 (1971).
[12]E. H. S. Burhop and W. N. Asaad, in *Advances in Atomic and Molecular Physics*, edited by D. R. Bates and I. Esterman (Academic, New York, 1972), Vol. 8, p. 163.
[13]C. P. Bhalla and M. Hein, Phys. Rev. Lett. 30, 39 (1973); C. P. Bhalla, N. O. Folland, and M. Hein, Phys. Rev. A 8, 649 (1973).
[14]C. P. Bhalla and D. L. Walters, U. S. Atomic Energy Commission Report CONF-720404, 1973 (unpublished).
[15]F. P. Larkins, J. Phys. B 4, L29 (1971).
[16]F. Herman and K. Schwarz, *Computational Solid State Physics* (Plenum, New York, 1972); F. Herman, I. B. Ortenburger, and J. P. Van Dyke, Int. J. Quantum Chem. 3, 827 (1970); Phys. Rev. Lett. 22, 807 (1969).
[17]J. S. Hansen, Bull. Am. Phys. Soc. 18, 663 (1973).
[18]Robert L. Kauffman, C. Fred Moore, Patrick Richard, and J. H. McGuire, Phys. Rev. A 8, 1233 (1973).
[19]J. D. Garcia, R. J. Fortner, and T. M. Kavanagh, Rev. Mod. Phys. 45, 111 (1973).
[20]C. E. Busch, A. B. Baskin, P. H. Nettles, S. M. Shafroth, and A. W. Waltner, Phys. Rev. A 7, 1601 (1973).
[21]G. Basbas, W. Brandt, R. Laubert, A. Ratkowski, and A. Schwarzschild, Phys. Rev. Lett. 27, 171 (1971).